IOPscience iopscience.iop.org

Home Search Collections Journals About Contact us My IOPscience

Breakdown of conductance quantization in quantum point contacts with realistic impurity potentials

This article has been downloaded from IOPscience. Please scroll down to see the full text article.

1995 J. Phys.: Condens. Matter 7 6253

(http://iopscience.iop.org/0953-8984/7/31/009)

View the table of contents for this issue, or go to the journal homepage for more

Download details:
IP Address: 171.66.16.151
The article was downloaded on 12/05/2010 at 21:51

Please note that terms and conditions apply.

J. Phys.: Condens. Matter 7 (1995) 6253–6270. Printed in the UK

Breakdown of conductance quantization in quantum point contacts with realistic impurity potentials

Alexandre M Zagoskin, Sergey N Rashkeev, Robert I Shekhter and Göran Wendin

Department of Applied Physics, Chalmers University of Technology and Göteborg University, S-41296 Göteborg, Sweden

Received 7 March 1995

Abstract. The breakdown of conductance quantization in a quantum point contact in the presence of a random long-range impurity potential is discussed. It is shown that in the linear response regime a decisive role is played by the indirect backscattering mechanism via quasilocalized states at the Fermi level; this can provide a much higher backscattering rate than any direct backscattering process. For realistic contact lengths ($\leqslant$2000 nm) the scattering processes prove to be independent, in spite of the coherence of the electron wave. The distribution function of conductance fluctuations is obtained by direct numerical calculations as well as being estimated within an analytical model for the first time. It is shown to be a generalized Poisson distribution. Estimates are made for quantum point contact performance at different choices of parameters. In particular, it is better the larger the intermode distance is compared to the amplitude of the random impurity potential.

1. Introduction

The effect of conductance $2e^2/h$ quantization in quantum point contacts (QPC, electrostatically defined junction in a two-dimensional electron gas in a high-mobility GaAs–AlGaAs heterostructure), first observed in 1988 [1], is still challenging both theoreticians and experimentalists [2]. An intriguing feature of the effect is that it is not destroyed by elastic scattering, be it impurity scattering or scattering by a contact boundary.

The insensitivity of quantization to the latter process was explained within the framework of the adiabatic approximation [3]. Breakdown of quantization was shown to be insignificant as long as the contact shape (i.e., the confining potential induced by the gate electrode) is smooth on the scale of Fermi wavelength, λ_F. The last condition is likely to be true, since $\lambda_F \simeq 40$ nm in a clean contact is at least an order of magnitude less than the characteristic scale of the gate potential variation [4].

The adiabatic approximation yields that different transverse modes pass the QPC independently ('no mode-mixing' regime). This provides a sufficient, but not necessary, condition for the conductance quantization in a QPC: as was pointed in [4, 5], the necessary condition is the absence of backscattering. The direct numerical calculations [6] show that conductance is quantized even if the intermode mixing is significant. The sum rule suggested there to explain this result follows from the unitarity of the scattering matrix of the system [7].

The impurity potential is more likely to produce backscattering, and thus to break the conductance quantization, since it is less smooth than the gate-induced potential. Many

0953-8984/95/316253+18$19.50 © 1995 IOP Publishing Ltd

theoretical papers dealing with impurity scattering in QPC [8, 9, 14] have used the Anderson model with on-site disorder. This approach gives a qualitative understanding of the process, but its results cannot be directly applied to real GaAs planar structures, where the Coulomb impurity potential certainly is not sharp on the scale of λ_F [4, 10]. In fact, the numerical calculations made for this realistic case [4] show that its scale of variation is intermediate between λ_F and the size of the QPC itself.

The effect of such a slowly varying random potential ('soft disorder') on the performance of a QPC was investigated in [4, 10]. Its main feature is the negligible rate of scattering processes with large momentum transfer. Glazman and Jonson [10] built up a theory for the electrical conductivity through the QPC with soft disorder and showed that the *direct backscattering* occurs mainly in the largest-number transverse mode (i.e., the one with the minimal longitudinal momentum). On the other hand, Laughton *et al* [4] demonstrated that the long-range impurity potentials may produce quasilocalized states inside the channel [11]. Once it has appeared, such a state provides an effective *indirect* backscattering mechanism. Indeed, the quasilocalized state contains both 'forward' and 'backward' waves, so that the transition between the electronic states propagating in opposite directions via the quasilocalized state does not demand a significant momentum transfer. Thus, in an appropriate impurity configuration, indirect backscattering (formally due to the second-order process) can have much larger cross-section than the (first-order) direct backscattering. The probability of finding such a configuration of impurities, of course, must be investigated as well. Recently Gurvitz and Levinson [12] built up a theory of resonant reflection and transmission in a QPC with a single attracting impurity at the contact's bottleneck. They have investigated the case when the first mode is open and a second one is being opened, thus creating a single resonant level at the top of the potential well. They obtained a Breit–Wigner-type expression for the correction to the conductance at the transition region from the first to second conductance step (as a function of the Fermi energy); its sign depends on whether there takes place tunnelling into the resonant state (conductance enhancement) or scattering into it (suppression).

In this paper we study numerically and analytically the indirect backscattering effects on the electrical conductivity of a QPC, in the presence of the screened Coulomb potential from randomly distributed charged impurities [13].

In section 2 we find the corresponding correction to the current, supposing that there are quasilocalized states in the QPC, and that the impurity potential is soft, so that the tunnelling processes to and from these states can be neglected, and their energetic spectrum is dense. We show that the correction, given by a Breit–Wigner-type formula, suppresses the current. If the quasilocalized states exist close to the Fermi surface, this is really the leading contribution from the impurity scattering in a QPC. The result is valid for the bulk of the conductance step against gate voltage.

In section 3 we investigate the stochastic properties of arising conductance fluctuations, as a random variable determined by the specific impurity arrangement. The distribution function of the conductance fluctuations is shown to be of Poisson type and is explicitly determined by the tunable parameters of the QPC: its length and number of open modes (i.e., conductance). This allows us to make more detailed predictions about the QPC performance than mere knowledge of the fluctuation dispersion.

In section 4 we estimate the theory parameters based on the quasiclassical description of the random impurity potential.

In section 5 we present the numerical calculations that provide the basis for the present work. The impurity potential was calculated in a self-consistent way using the Thomas–Fermi approximation. The quantum contact was modelled by imposing upon it a parabolic

confining potential. The conductance was calculated in the linear-response limit by a standard transfer matrix method for different contact lengths and for different realizations of the impurity potential. (Different realizations of the random impurity potential in the QPC were obtained by changing the position of the confining potential with respect to a fixed random potential profile.)

An empirical distribution function of conductance fluctuations was thus obtained, and we compare the results of the numerical calculations and theoretical predictions in section 6. They are in very good agreement. This allows us to conclude that the leading mechanism of conductance quantization breakdown in QPCs is the indirect backscattering, and it allows us to find estimates of the QPC performance.

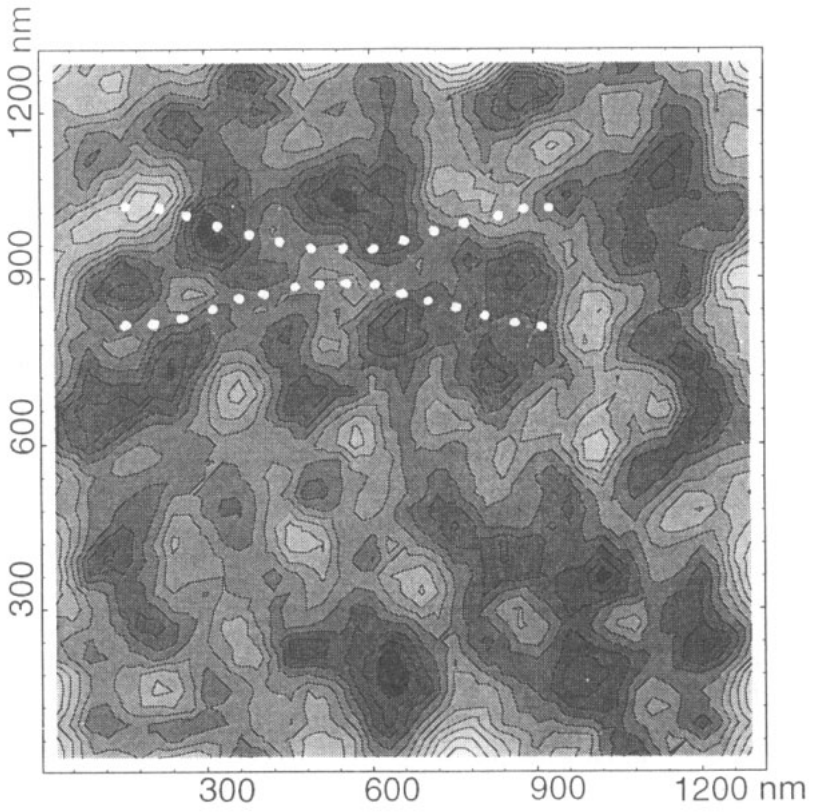

Figure 1. The model of a quantum point contact. The impurity potential in a 2DEG layer. The impurity density is 10^{12} cm^{-2}. Isolines are drawn through 1.3×10^{-3} eV. The white line shows the gate equipotential $U_g^{(0)}(x, y) = E_F$ (unperturbed contact shape) for $L = 800$ nm.

2. Indirect backscattering in a quantum point contact

In accordance with what is now the standard approach [3, 10], we start from the adiabatic model of a QPC, where the transverse modes are well defined; the deviations will be regarded as a perturbation (see figure 1). The Hamiltonian of the electron contains the

following terms:

$$H = -\frac{\hbar^2}{2m^*}\left(\frac{\partial^2}{\partial x^2} + \frac{\partial^2}{\partial y^2}\right) + U_g(x, y) + V(x, y). \tag{1}$$

Here $U_g(x, y)$ is the confinement potential, shaping the junction in a two-dimensional electron gas (2DEG). It proves to be convenient to include the smooth component of the impurity potential as well. The rest of the impurity potential, $V(x, y)$, is regarded as a perturbation, e.g., leading to intermode mixing. It is also a soft potential, which does not lead to large momentum transfer.

The potential $U_g(x, y)$ is supposed to be a slow function of the coordinates. Then the wave function of an electron with energy E inside the QPC can be expanded as follows [3]:

$$\Psi(x, y; E) = \sum_{m,\alpha} C_{m,\alpha}\psi_{m,\alpha}(x, y; E). \tag{2}$$

The adiabatic eigenfunctions are defined by

$$\psi_{m,\alpha}(x, y; E) = \phi_m(x, y)\chi_{m,\alpha}(x; E) \tag{3}$$

where the transverse eigenfunction corresponds to the mth eigenvalue of the transverse Hamiltonian:

$$H_\perp\phi_m(x, y) \equiv \left\{-\frac{\hbar^2}{2m^*}\frac{\partial^2}{\partial y^2} + U_g(x, y)\right\}\phi_m(x, y) = E_{m\perp}(x)\phi_m(x, y) \tag{4}$$

and the longitudinal eigenfunction satisfies the equation

$$\left\{-\frac{\hbar^2}{2m^*}\frac{\partial^2}{\partial x^2} + E_{m\perp}(x)\right\}\chi_{m,\alpha}(x; E) = E\chi_{m,\alpha}(x; E). \tag{5}$$

We can distinguish different groups of electronic states in the QPC, according to the behaviour of $\chi_{m,\alpha}(x; E)$ in the presence of the effective one-dimensional potential $E_{m\perp}(x)$ (see figure 2). They are denoted by the index $\alpha = -2, -1, \ldots, 2$.

The states of special interest for us are the quasilocalized ones ($\alpha = 0$). They appear if the effective potential $E_{m\perp}(x)$ is a nonmonotonic function. Note that for each quasilocalized state in the mth mode, generally, there exist propagating states with the same energy in some mode of lower number (figure 2). This is the reason why these states are *quasi*localized (due to the smoothness of the potentials in the QPC we can safely neglect another reason for this, namely, the tunnelling decay).

The coexistence of propagating and quasilocalized states (P states and Q states) at the same energy is characteristic for QPCs and gives rise to indirect backscattering in the QPC.

The correction to the current due to backscattering can be written in a standard way [3, 17]:

$$\Delta I = -\frac{2|e|}{h}\int \mathrm{d}E\ (n_F(E - \mu_1) - n_F(E - \mu_2))\, J(E) \tag{6}$$

$$J(E) = \sum_{m=1}^{N}\sum_{n=1}^{N}|r_{nm}(E)|^2. \tag{7}$$

In the linear-response limit this yields the correction to the conductance,

$$\Delta G = -\frac{2e^2}{h}J(E_F). \tag{8}$$

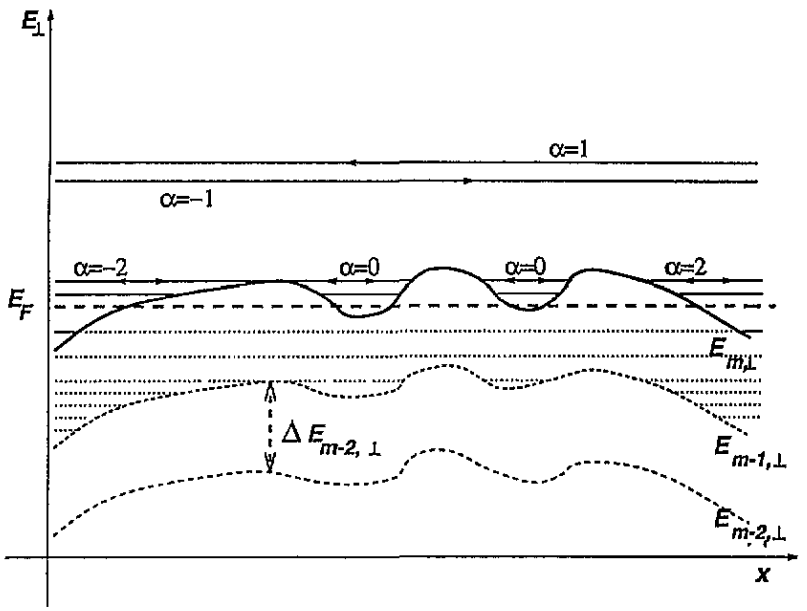

Figure 2. Classification of electronic states in a QPC. $E_{m\perp}(x)$, effective potential in mth mode (1D subband). ($\alpha = -2$), reflected states incident from the left; ($\alpha = -1$), propagating states incident from the left; ($\alpha = 0$), quasilocalized states; ($\alpha = 1$), propagating states incident from the right; ($\alpha = 2$), reflected states incident from the right.

The summation in (7) is taken only over N propagating (open) modes in the quantum point contact, and $r_{nm}(E)$ is the probability amplitude of the electron incident from the right in the mth P mode ($\alpha = 1$) to be scattered back, to the nth P mode with $\alpha = -1$:

$$r_{nm}(E)\,\delta(E - E') = \left(\psi_{n,-1}(E'),\, \Psi^{out}_{m,1}(E)\right). \tag{9}$$

Here $\Psi^{out}_{m,1}(x, y; E)$ is the scattered wave, corresponding to the unit wave with energy E, incident from the right in the mth mode, $\psi_{m,1}(x, y; E)$. This function can be found from the Lippmann–Schwinger equation [18] ($r = (x, y)$):

$$\Psi^{out}_{m,1}(r; E) = \psi_{m,1}(r; E) + \int \mathrm{d}r'\, G^R(r, r'; E) V(r') \psi_{m,1}(r'; E). \tag{10}$$

In this equation we have introduced the exact retarded Green function in the presence of the perturbation $V(x, y)$, for which we can write

$$G^R(r, r'; E) = G^R_0(r, r'; E) + \int \mathrm{d}r''\, G^R_0(r, r''; E) V(r'') G^R_0(r, r'; E) + \cdots. \tag{11}$$

The unperturbed retarded Green function is given by

$$G^R_0(r, r'; E) = \sum_{m,\alpha,\epsilon} \frac{\psi_{m,\alpha}(r; \epsilon)\psi^*_{m,\alpha}(r'; \epsilon)}{E - \epsilon + \mathrm{i}0} \equiv \sum_{\alpha} G^{R;\alpha}_0(r, r'; E). \tag{12}$$

The summation is taken over all the quantum numbers of electronic unperturbed eigenfunctions.

Inserting equations (10), (11) into (9) we find the first two nonvanishing terms:

$$r_{nm}(E)\,\delta(E - E') = \left(\psi_{n,-1}(E'), G^R_0(E) V \psi_{m,1}(E)\right) + \left(\psi_{n,-1}(E'), G^R_0(E) V G^R_0(E) V \psi_{m,1}(E)\right). \tag{13}$$

We neglect the higher-order terms which implies, in particular, that the scattering processes by different quasilocalized levels do not interfere. This approximation is surely valid if $L \ll l_{tr}, l_{loc}$, where l_{tr}, l_{loc} are the transport and localization lengths, respectively. The following results show that this condition holds in the case of realistic quantum contacts.

According to our initial assumptions, the perturbation potential is soft. This means that, generally, its matrix elements between the P states propagating in opposite directions (i.e., with $\alpha = +1$ and -1) are negligible, while the matrix elements between the P states and Q states ($\alpha = \pm 1$ and 0) are nonzero. Since the retarded Green function (12) contains the products of electronic eigenfunctions with the same indices α, equation (13) reduces to

$$r_{nm}(E)\,\delta(E-E') = \left(\psi_{n,-1}(E'), G_0^{R;-1}(E) V G_0^{R;0}(E) V \psi_{m,1}(E)\right). \tag{14}$$

The superscripts in the retarded Green functions show which part of the expansion (12) we keep.

The formula (14) shows that the backscattering from the incident $(m,1)$ state to the $(n,-1)$ state occurs through the set of quasilocalized states (described by part of the retarded Green function, denoted by $G_0^{R;0}(E)$).

After some standard transformations, we obtain that

$$r_{nm}(E) = 2\pi\nu(E) \sum_{q,\epsilon} \frac{(n;-1;E|\,V\,|q;0;\epsilon)\,(q;0;\epsilon|\,V\,|m;1;E)}{E-\epsilon+\mathrm{i}0}. \tag{15}$$

Here we have introduced the one-dimensional electronic density of states (DOS) at infinity, $\nu(E)$, to account for the propagating modes, and denoted the matrix elements of the perturbation potential by

$$(n;-1;E|\,V\,|q;0;\epsilon) \equiv \int \mathrm{d}r\, \psi^*_{n,-1}(r;E) V(r) \psi_{q,0}(r;\epsilon). \tag{16}$$

The summation is now taken only over the quasilocalized states; as such, they have a discrete spectrum, so that ϵ is a discrete variable; q is the number of transverse mode where the localized state appears.

Equation (15) contains the unperturbed retarded Green function of the electron in localized states, which thus have an infinite lifetime. The perturbation, mixing different states, makes the Q states metastable, and instead of the i0 term there appears the spectral function $\mathrm{i}\Gamma_q(\epsilon,\epsilon)/2$ [18] (the accompanying shift of the energy levels can be accounted for by changing the summation variable ϵ). The spectral function is given by

$$\Gamma_q(\epsilon,\epsilon') = 2\pi \sum_n \sum_{\alpha=\pm 1} \left|(q;0;\epsilon|V|n;\alpha;\epsilon')\right|^2 \nu(\epsilon) \tag{17}$$

(of course, a Q state can decay only into P states).

The correction to the current (6) is expressed through $J(E) = \sum_{m,n} |r_{nm}(E)|^2$. Note that the matrix elements corresponding to the Q states from different subbands ($q \neq q'$) or different impurity potential wells in the same subband ($w \neq w'$, where w is the label of the potential well) enter the expression for $r_{nm}(E)$ with their phases, which are uncorrelated. This means that the main contribution to $J(E)$ will be given by the diagonal terms in the corresponding sum, that is, as it is easily seen,

$$\begin{aligned} J(E) \simeq 4\pi^2\nu^2(E) \sum_{q,w} \sum_{\epsilon,\epsilon'} \Bigg[\sum_{m,n} & (n;-1;E|\,V\,|q;0;\epsilon)\,(q;0;\epsilon|\,V\,|m;1;E) \\ & \times (n;-1;E|\,V|q;0;\epsilon')(q;0;\epsilon'|V\,|m;1;E) \Bigg] \\ & \times \left[\left(E-\epsilon+\mathrm{i}\Gamma_q(\epsilon,\epsilon)/2\right)\left(E-\epsilon'-\mathrm{i}\Gamma_q(\epsilon',\epsilon')/2\right)\right]^{-1}. \end{aligned} \tag{18}$$

Here ϵ, ϵ' are different quasilocalized states in the *same* potential well of the *same* 1D subband.

This expression can be further simplified, if the distances between the energy levels in a potential well are large comparatively to their width: $\Delta\epsilon_{well} \gg \Gamma$. Then in the sum over ϵ, ϵ' in (18) the contribution of the terms with $\epsilon = \epsilon'$ is dominant, and we obtain

$$J(E) \simeq 4\pi^2\nu^2(E) \sum_{q,w,\epsilon} \frac{\sum_{m,n} |(n;-1;E|\,V\,|q;0;\epsilon)|^2\,|(q;0;\epsilon|\,V\,|m;1;E)|^2}{(E-\epsilon)^2 + (\Gamma_q(\epsilon,\epsilon)/2)^2}$$

$$= \sum_{q,w,\epsilon} \frac{(\Gamma_q(\epsilon,E)/2)^2}{(E-\epsilon)^2 + (\Gamma_q(\epsilon,\epsilon)/2)^2}. \tag{19}$$

The result has a typical Breit–Wigner form for a set of independent resonant levels [18], which is the case under the assumptions made.

Though the energy spectrum of the Q states in a single potential well is assumed to be rarified, in a long contact, where many potential wells with random parameters appear, and due to the fact that each Q state has a finite width Γ, the spectrum of these states for the whole system is dense enough to be described in a continuous approximation. Then we can introduce the density of localized states in the qth mode, $\aleph_q(\epsilon)$, and rewrite (19) as

$$J(E) = \sum_q \int \mathrm{d}\epsilon\, \frac{\aleph_q(\epsilon)(\Gamma_q(\epsilon,E)/2)^2}{(E-\epsilon)^2 + (\Gamma_q(\epsilon,\epsilon)/2)^2} \simeq \frac{\pi}{2} \sum_q \aleph_q(E)\Gamma_q(E,E). \tag{20}$$

In the linear-response limit this directly gives the correction to the conductance:

$$\Delta G \simeq -\frac{2e^2}{h}\frac{\pi}{2} \sum_q \aleph_q(E_F)\Gamma_q(E_F,E_F). \tag{21}$$

We have discussed only virtual (including resonant) scattering to and from the Q states. In reality, when the finite driving voltage U is applied, there exist the processes of *real* elastic and inelastic (electron–electron or electron–phonon) scattering between Q and P states with energies in the interval eU around the Fermi energy. The contribution of these states to the scattering is proportional to eU. We can safely neglect their existence in the linear-response limit $eU \to 0$, when the contribution from the Q states outside the eU band (in the interval of width $\sim \Gamma(E_F,E_F)$) is dominant. These kinetic processes, of course, must be taken into account if we would like to discuss the nonlinear response of a QPC.

3. Statistics of conductance fluctuations

Now let us discuss what the formula (21) yields. The conductance quantization breakdown can be characterized by the relative difference between the actual conductance against gate voltage dependence, $G(V_g)$, and the ideal one, averaged over the nth step (figure 3, inset) (reduced conductance deviation):

$$g_n = \left(2e^2/h\right)^{-1} \left(\int_{V_g(n)}^{V_g(n+1)} \mathrm{d}V_g\, |\Delta G(V_g)| \right) / [V_g(n+1) - V_g(n)]. \tag{22}$$

Inserting here (21), we get

$$g_n = \frac{\pi}{2} \sum_q \int_{V_g(n)}^{V_g(n+1)} \mathrm{d}V_g\, \aleph_q(E_F) \frac{\Gamma_q(E_F,E_F)}{V_g(n+1) - V_g(n)} \tag{23}$$

where the nth mode opens at the gate voltage equal to $V_g(n)$, and $\aleph_q(E_F)$ and $\Gamma_q(E_F,E_F)$ are both dependent on V_g. In the last equation we can instead of integrating over the gate

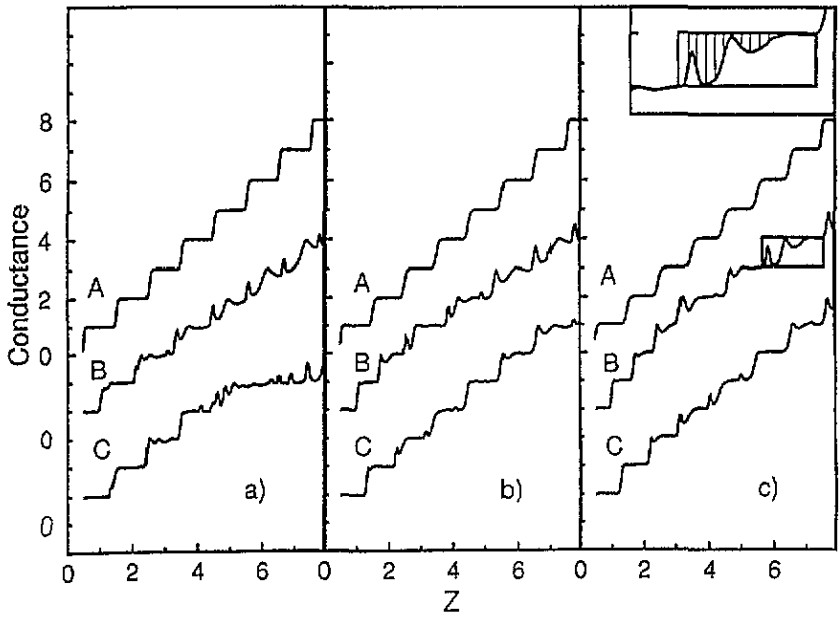

Figure 3. Conductance against gate voltage curves for different realizations and contact lengths (see text). Parameter $Z = k_F b(0)/\pi$. (a) Contact length 1200 nm, (b) 800 nm, (c) 600 nm. Inset: quantization breakdown parameter g; it is equal to the ratio of the area of the dashed part of the conductance step to its total area.

voltage integrate over the (determined by V_g) transverse subband energies at some point x_0 of the constriction, $E_{q,\perp}(x_0) \equiv E_{q,\perp}$. The integral evidently does not depend on x_0. The intermode distance, $\Delta E_{q,\perp}(x_0) = E_{q+1,\perp}(x_0) - E_{q,\perp}(x_0) \equiv \Delta E_{q,\perp}$ (see figure 2), weakly changes when the gate voltage changes between $V_g(n)$ and $V_g(n+1)$. (The direct measurements show that the main effect of the gate voltage is an upward shift of the potential in the centre of the constriction [20].) In the realistic model of a parabolic confining potential the intermode distance also does not depend on the mode number. In long smooth contacts it is weakly dependent on the longitudinal coordinate as well. Its magnitude is of the order of E_F/N_{max}, where N_{max} is the maximum number of transverse modes able to pass the constriction (which is the maximum number of conductance $2e^2/h$ steps which can be observed in a given QPC). This enables us to simplify equation (23):

$$g_n \approx \frac{\pi}{2} \sum_q \int_{E_{q\perp}}^{E_{q\perp}+\Delta E_\perp} \mathrm{d}E_\perp \, \aleph_q(E_F) \frac{\Gamma_q(E_F, E_F)}{\Delta E_\perp}. \tag{24}$$

The functions under the integral are now functions of the corresponding transverse energies.

If localized states have an almost continuous spectrum (which is consistent with our initial assumption of the impurity potential being smooth), the main dependence on the bottom energy of the mode enters the DOS, not the level width, which is a smooth function of energy in the scale of $\Delta E_\perp$. Therefore, we can take it out from the integral. Then we obtain the following formula:

$$g_n \approx \frac{\pi}{2} \frac{\Gamma(E_F, E_F; n)}{\Delta E_\perp} \int_{E_{q\perp}}^{E_{q\perp}+\Delta E_\perp} \mathrm{d}E_\perp \sum_q \aleph_q(E_F). \tag{25}$$

Here we explicitly show that, as follows from the definition (17), $\Gamma_q(E_F, E_F)$ depends on the number of propagating states in the contact, that is, on the step number n.

Assuming that the quantity $\pi\Gamma(E_F, E_F; n)/2\Delta E_\perp$ is slightly dependent on the realization of the random potential, we can substitute it by its ensemble average value,

$$\Delta g_n = \frac{\pi\langle\Gamma(E_F, E_F; n)\rangle}{2\Delta E_\perp} = \gamma n \tag{26}$$

which is proportional to the number of open modes, n (see (17)).

The integral over energy in (25) has the sense of the *number of localized states* in all 1D subbands in the contact, which pass the Fermi level as we sweep V_g across the nth conductance step, N_Q. We denote its average over possible realizations of the random potential by κL (L is the length of the contact):

$$\kappa = \frac{\langle N_Q\rangle}{L} = \frac{1}{L}\int_{E_{q\perp}}^{E_{q\perp}+\Delta E_\perp} \mathrm{d}E_\perp \left\langle \sum_q \aleph_q(E_F)\right\rangle \tag{27}$$

or

$$\kappa = \int_{E_{q\perp}}^{E_{q\perp}+\Delta E_\perp} \mathrm{d}E_\perp \left\langle \sum_q \mathcal{N}_q(E_F)\right\rangle. \tag{28}$$

Here $\langle\mathcal{N}_q(E)\rangle$ is the ensemble average of DOS *per unit length* in the qth 1D subband over possible realizations of the random impurity potential.

The expression (25) acquires a clear physical meaning. The correction to the contact conductance due to indirect backscattering is a sum of contributions, Δg_n, (see equation (26)) from independent Q states (in each 1D subband):

$$g_n = N_Q\Delta g_n. \tag{29}$$

In the limit of infinitely long quantum contact we get

$$\lim_{L\to\infty}\frac{\aleph_q(E)}{L} = \langle\mathcal{N}_q(E)\rangle \Rightarrow \lim_{L\to\infty}\frac{N_Q}{L} = \kappa \tag{30}$$

since the density of states is the self-averaging quantity [19]. But in the contact of finite length the number of appropriate Q states deviates from its ensemble average, $\langle N_Q\rangle = \kappa L$, and thus the conductance of the QPC will fluctuate from realization to realization. In order to predict the performance of a single QPC, we need the distribution function of these fluctuations, dependent on such parameters of the contact as its length L and number of open modes n.

On a length scale large compared to the size of the localized state (correlation radius of the impurity potential of order 100 nm), we can regard these states as *independently randomly distributed along the channel, with occurrence per unit length* κ. The probability of finding p such states along the total length L of the contact is then given by the Poisson formula [21]:

$$\Pi(N) = (\kappa L)^N e^{-\kappa L}/N!\,. \tag{31}$$

Since each state gives the same contribution to the conductance, $\Delta g_n = \gamma n$, then the probability *density* of the conductance deviation on the nth step

$$P(g_n = N\gamma n) = \frac{(\kappa L)^{g/\gamma n}\,\mathrm{e}^{-\kappa L}}{\gamma n\,(g/\gamma n)!}. \tag{32}$$

The reduced conductance deviation acquires the discrete set of values $g_n = \gamma n$, $2\gamma n$, $3\gamma n$, ..., depending on the number of relevant Q states in the contact.

The shortcoming of the above formula (discrete set of values of g_n) follows from our simplifying assumption that each Q state has the same width $\langle\Gamma(E_F, E_F)\rangle$. In reality, this

quantity also fluctuates, so that the variable g_n is rather a continuous one. Nevertheless, as the numerical calculations show, this expression provides a fairly good description of the performance of a QPC (see section 6).

4. Estimates of the theory parameters

We see that the statistics of the conductance fluctuations due to indirect backscattering is determined by the following parameters (see equation (32)): effective length of the QPC, L, number of open modes, n, average 1D density of Q states at the Fermi energy per unit length, κ, and average contribution to the conductance from each Q state, Δg. Since the latter quantity is proportional to the average scattering rate from these states to the propagating ones (see equation (26)), it is more convenient to use the set of four independent parameters, L, n, κ and γ.

The first two are *tunable parameters*, which can be changed by changing V_g and/or gate configuration, while the other two are essentially determined by the properties of a given GaAs structure (density and charge of impurities, spacer thickness etc), or, in short, by the impurity potential in the system. We need some numerical estimates for these *intrinsic parameters*, γ and κ. They can be obtained from such characteristics of the impurity potential as its correlation length, l_V, and dispersion, $\sigma^2 \equiv \langle V_{imp}^2 \rangle$, which are both contained in the correlation function $K(x)$ or spatial spectral density $S(k)$ (see [19]):

$$K(x) = \langle V_{imp}(0) V_{imp}(x) \rangle \qquad S(k) = \int \mathrm{d}^d x \, K(x) \mathrm{e}^{-\mathrm{i}k \cdot x}. \tag{33}$$

(We put to zero the average value of the impurity potential.)

First we estimate γ. Since $\langle \Gamma(E_F, E_F) \rangle \simeq 2\pi n 2\nu \overline{|\langle Q|V|P\rangle|^2}$ (see (17)), then

$$\gamma \simeq 2\pi^2 \nu \overline{|\langle Q|V|P\rangle|^2} / \Delta E_\perp. \tag{34}$$

Here $\overline{|\langle Q|V|P\rangle|^2}$ is the average square modulus of the impurity potential between quasilocalized and propagating states. Evidently, it is of the order of $S(\Delta k_{PQ})\alpha^2 / l_0$, where Δk_{PQ} is the difference of longitudinal wave vectors in P and Q states, α is the reduced matrix element of impurity potential between different transverse modes ($\alpha \simeq 0.1$ according to our numerical calculations, see section 5), and $l_0 \simeq l_V$ is the average longitudinal size of the quasilocalized state (the latter factor appears because the wave functions of Q states are normalized to unit *probability*, while the P states are normalized to unit *probability current* along the axis of the QPC). In accordance with our basic assumptions, for the relevant (Q,P) matrix elements of the impurity potential the longitudinal wavevectors are almost the same: $\Delta k_{PQ} \ll k_F$. Assuming the exponential potential decay, we can take

$$\overline{|\langle Q|V|P\rangle|^2} \simeq S(0)\mathrm{e}^{-2\Delta k_{PQ} l_V} \alpha^2 / l_V = S(0)\mathrm{e}^{-4\pi (l_V/\lambda_F)(\Delta k_{PQ}/k_F)} \alpha^2 / l_V \leqslant \sigma^2 l_V \alpha^2. \tag{35}$$

This gives the following estimate for γ:

$$\gamma \leqslant 2\pi^2 \alpha^2 \frac{\sigma^2}{E_F \, \Delta E_\perp} \frac{l_V}{\lambda_F}. \tag{36}$$

We use here the formula for 1D DOS of propagating states, $\nu = 1/\pi\hbar v_F$.

If we insert into (36) the values consistent with our numerical calculations, $\alpha = 0.1$, $\lambda_F = 40$ nm, $l_V = 100$ nm, $\sigma^2 = 0.1E_F^2$, $\Delta E_\perp = 0.3E_F$, then we obtain $\gamma \leqslant 0.15$. This is a proper order of magnitude estimate, though higher than the value that follows from the numerical calculations (see section 6). The reason is that, putting $\Delta k_{PQ} = 0$ in (35), we overestimated γ. To eliminate this discrepancy, it is sufficient to take $\Delta k_{PQ}/k_F \simeq 7\%$, which is quite reasonable.

One useful remark: we can approximately present the impurity potential as a sum of potentials of identical potential centres, $v(x)$, with density n_{imp} randomly distributed in the conducting plane (see, e.g., [19]). Then by the Carson theorem we get [21] $S(k) = n_{imp}|v(k)|^2$. Therefore, the parameter γ is proportional to the impurity density.

In order to estimate the other intrinsic parameter, κ, we use the quasiclassical, or Thomas–Fermi, approximation for the average density of localized states in the 1D subband, $\langle \mathcal{N}(E) \rangle$ (see [19]), leading to the following approximate expression:

$$\langle \mathcal{N}_q(E,x) \rangle = \frac{\sqrt{m}}{\pi\hbar\sqrt{\sigma}}\theta(E_{q\perp}(x)-E)\exp\left(-\frac{\left(E_{q\perp}(x)-E\right)^2}{4\sigma^2}\right)\mathrm{D}_{-1/2}\left(\frac{E_{q\perp}(x)-E}{\sigma}\right)$$
$$\approx \frac{\theta(E_{q\perp}(x)-E)}{\sqrt{E_{q\perp}(x)-E}}\frac{\sqrt{m}}{\pi\hbar}\exp\left(-\frac{\left(E_{q\perp}(x)-E\right)^2}{2\sigma^2}\right). \tag{37}$$

$\mathrm{D}_{-1/2}(z)$ is the parabolic cylinder function. As a matter of fact, the validity limits of the latter expression are determined not by the quasiclassicity conditions, but by much looser ones [19]:

$$|E - E_{q\perp}(x)| \gg \sigma, E_F\frac{\lambda_F^2}{l_V^2}. \tag{38}$$

Substituting it into the definition of κ (28), we find

$$\kappa \approx \sum_q \int_{E_{q\perp}}^{E_{q\perp}+\Delta E_\perp} \mathrm{d}E\,\frac{\theta(E-E_F)}{\sqrt{E-E_F}}\frac{\sqrt{m}}{\pi\hbar}\mathrm{e}^{-[(E-E_F)^2/2\sigma^2]}$$
$$\approx \int_{E_F+\Delta E_\perp}^{\infty}\frac{\mathrm{d}E}{\Delta E_\perp}\Delta E_\perp\frac{1}{\sqrt{E-E_F}}\frac{\sqrt{m}}{\pi\hbar}\mathrm{e}^{-[(E-E_F)^2/2\sigma^2]}. \tag{39}$$

The latter formula can be identically rewritten as follows:

$$\kappa \approx 2^{-1/4}\Gamma\left(\frac{1}{4},\frac{1}{2}\left(\frac{\Delta E_\perp}{\sigma}\right)^2\right)\sqrt{\frac{\sigma}{E_F}}\frac{1}{\lambda_F}. \tag{40}$$

Here $\Gamma(\alpha,z) = \int_z^\infty \mathrm{d}y\, y^{1-\alpha}\mathrm{e}^{-y}$ is the incomplete gamma function.

With the same choice of parameter values as above, we find that $\kappa \simeq \sqrt{0.66}\ \Gamma(\frac{1}{4},\frac{1}{2})/\lambda_F = 0.269/\lambda_F \approx 0.006\ \mathrm{nm}^{-1}$.

5. Numerical calculations

The basis for our hypothesis about the statistics of conductance deviations from ideal quantization is the numerical calculations of QPC conductance for different realizations of soft random impurity potential, at different contact lengths and for different number of open modes.

The model used for simulation of a heterostructure device is very similar to the one considered in [4]. Donors are assumed to be fully ionized and distributed randomly through the donor layer. We restricted donors to a plane which should be considered as the middle of the donor layer. In our calculations all the donors in the n-type $Al_xGa_{1-x}As$-doped layer have the same height $h = 30$ nm above the 2DEG. The electrons are treated as a two-dimensional layer of 10 nm thickness, which is much smaller than other relevant length scales. The positions of the impurities were generated by the uniform random number generator on the square $1290 \times 1290\ \mathrm{nm}^2$. We assumed periodic boundary conditions, i.e. this square was continued periodically in all directions in the 2D plane. In order to avoid the

occasional appearance of too dense clusters of impurities in the donor plane the distribution of impurities has been 'relaxed', namely, we did not allow the appearance of more than five impurity atoms at the area $1/n$, where n is the 2D concentration of impurities. For the realistic concentration of impurities, $n = 10^{12}$ cm^{-2}, one must discard not more than 5–10% of impurities. The potential of a single impurity was taken in the following form:

$$v(r - r_i) = \frac{e}{\varepsilon\sqrt{(r - r_i)^2 + h^2}} \tag{41}$$

where ε ($\approx$13) is the static dielectric function of GaAs, r is the position vector in the 2D plane, and r_i is the coordinate of the ith impurity. Since we did not want to be too specific in modelling any definite heterostructure, we did not take into account the image term considered in [4].

The potentials of the impurities were summed directly. The numerical calculations show that the summation of the potentials of impurities situated within the radius $|r - r_i| \leqslant r_{max} = 10h$ gives the resulting potential with a good precision. For the rest of the plane the summation could be substituted by integration over a plane with homogeneously distributed charge. This gives a constant term, which can be dropped since we are only interested in the fluctuations of the impurity potential around its average value. Therefore, we choose the average value of the summed potential as a point of reference for the energy, i.e. we take $\langle V_{imp}\rangle = 0$. Further increase of r_{max} does not give any significant change for the potential fluctuations defined in such a way.

The amplitude of fluctuations of the *unscreened* impurity potential proves to be too large, for a realistic concentration of impurities $n \sim 10^{12}$ cm^{-2} being a few times greater than the Fermi energy (of the order of 10^{-2} eV). This means that the screening of this potential by the electrons in the 2DEG should necessarily be taken into account. For a qualitative estimation of this effect we used the way proposed in [4]: the Thomas–Fermi approximation, which is applicable in the case of slowly varying (on the scale of λ_F) impurity potential, i.e., our case. The density of electrons is then given by the local equation

$$n(r) = \frac{m^*}{\pi\hbar^2}(\mu - eV_{tot}(r))\theta(\mu - eV_{tot}(r)) \tag{42}$$

where μ is the chemical potential, and V_{tot} is a sum of the unscreened impurity potential and the induced potential from the electrons in the 2DEG,

$$V_{tot} = V_{imp} + V_{ind}. \tag{43}$$

V_{ind} is related to n_{ind} by the Poisson equation. For a fixed chemical potential equations (42) and (43) give a possibility of finding the total potential V_{tot} in a self-consistent manner. One must keep in mind that the experimentally observed Fermi energy should be measured from the average total potential, namely, one more equation should be added to this self-consistent scheme,

$$E_F = \mu - \langle V_{tot}\rangle. \tag{44}$$

Here $\langle V_{tot}\rangle$ is the average total potential, E_F is considered as a fixed parameter given by the experiment, μ is the 'bare' chemical potential. It shows the degree of filling of the system by electrons and varies from iteration to iteration. Obviously, this system of equations has a single self-consistent solution. The numerical calculations show that for $n \sim 10^{12}$ cm^{-2} and $E_F \simeq 10^{-2}$ eV this solution is achieved when the system is almost completely filled by the electrons, i.e., for most of the points in the 2D plane n_{ind} is nonzero and the resulting potential fluctuations are smaller than (or of the order of) the Fermi energy,

$V_{tot} - \langle V_{tot} \rangle \leqslant E_F$ (see figure 1). The characteristic scale of the change of the potential fluctuation is of the order of 100–200 nm.

The calculations of the potential were made with a crude mesh in the 2D plane. To solve the scattering problem by the standard transfer matrix method, a finer mesh is desirable, and the potential was therefore interpolated by the cubic splines when necessary.

In all these considerations we did not take into account the self-consistent effects of redistribution of electrons in the constriction due to the gate voltage. Nevertheless, it is clear that such effects could be very significant, since they could enhance the potential of a single impurity located in a bottle neck because the concentration of electrons in this area is lower than the average one, and screening is suppressed (impurity denudation effect). Such an effect increases the potential fluctuations at the bottle neck and can change significantly the whole behaviour of the conductance (locking the channel) [4]. The question of how this effect of just a few impurities located at the narrowest place may show up in the statistics of conductance fluctuations is still open. We plan to discuss such a challenging subject elsewhere.

In order to obtain the transmittance and reflectance matrices we solved the 2D Schrödinger equation rewriting it in matrix form by the standard transfer matrix method with the proper boundary conditions. In order to model the gate voltage we used a parabolic potential, as in [6],

$$U_g(x, y) = \hbar^2\eta^2/2m^*[2y/b(x)]^2 \tag{45}$$

where $\eta = \pi k_F/4$, and

$$b(x) = b_\infty - (b_\infty - b_0)\sin^2(\pi x/L) \qquad -L/2 \leqslant x \leqslant L/2. \tag{46}$$

We chose the parameters $b_0 = 10$ nm and $b_\infty = 170$ nm, i.e., the maximum number of the modes passing through the constriction is eight, for the realistic $\lambda_F = 42$ nm.

As long as we are interested mostly in long constrictions (of length 600 nm and longer) this impurity scattering term will be dominant in comparison with effects of changes of the width $b(x)$ along the constriction, a case thoroughly considered by Brataas and Chao [6] for short contacts. In the bulk of our calculations we neglect them. Because the most important region for the breakdown of quantization lies near the bottleneck, we multiply the impurity potential inside the contact by the factor $\sin^2(\pi x/L)$. This gives us the freedom not to care about changing the boundary conditions for any realization of the potential. The number of entering modes is always constant.

The statistics of conductance deviations in quantum contacts can be obtained either (i) by generating the impurity potential (with the self-consistent procedure) for each realization of the constriction, or (ii) by moving the centre of the contact (possibly also changing the direction of the axis of the contact) over the plane with the impurity potential obtained in a self-consistent manner only once. The second way is surely less time consuming and, therefore, is the one we use.

We performed numerical calculations for contacts of three lengths (600, 800 and 1200 nm) for 625 different realizations of impurity potential, moving the centre of the X-oriented contact on the square of 1290×1290 nm^2, with the periodic boundary conditions described above.

We also calculated the conductance of very long QPCs (up to 10 000 nm) for several realizations.

6. Analysis of the results

The results of the calculations are shown in figures 3, 4 and 5. Typical conductance against gate voltage curves are shown in figure 3. Curves A correspond to an impurity-free contact. The centre of the contact lies at the same place for all the curves B (at a minimum (valley) of the impurity potential) and C (at a maximum (hill)). Evidently the C curves demonstrate better quantization than the B curves, for the same contact length and step number. This agrees with our statement that the indirect backscattering is a more effective mechanism of quantization breakdown in QPCs. The quantization quality becomes poorer for larger contact length and higher step number.

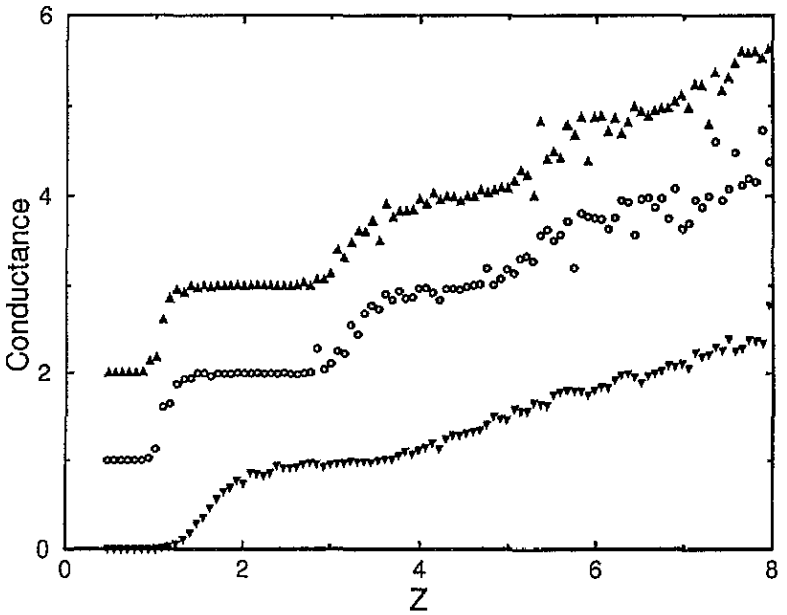

Figure 4. Conductance against gate voltage curves for three different realizations for the contact length $L = 10\,000$ nm (see text). The random potential has been generated on the rectangle $1290 \times 12\,900$ nm^2 for these calculations.

The conductance against gate voltage curves in a very long QPC ($L = 10\,000$ nm) for three different realizations are shown in figure 4. We would like to note here that no trace of localization in the system is detected. On the other hand, the conductance plateaus (except the first one) are totally destroyed at this length.

In order to obtain more convincing proof of our theory, the statistics of conductance fluctuations was investigated. The average conductance deviation from the ideal conductance step, g, was calculated in 625 realizations for each step ($n = 2, 3, \ldots, 6$) and each contact length ($L = 600$, 800, 1200 nm), and the empirical distribution function was obtained:

$$P_{emp}(g)\,\delta g = N(p\,\delta g)/625 \tag{47}$$

where $N(p\,\delta g)$ is the number of realizations for which $p\,\delta g \leqslant g < (p+1)\,\delta g$. In the actual calculations $\delta g = 0.02$.

Since the contact has a finite length, the deviation g is finite even without impurities due to the geometric step smoothening [22]; it is larger the shorter the contact is. Therefore when

calculating g, we have subtracted from it the corresponding value of g for the impurity-free case.

The average deviation increases with the mode number and the contact length. The empirical distributions are essentially asymmetric. Some of them have a tail stretching into the negative-g region. This means that in some cases the impurity potential can make the contact more transparent in comparison with the case without impurities. There may be two mechanisms for this transparency growth. First, there may occur tunnelling through the localized states in the transition regime, which enhances the contact transparency [12]; second, the random impurity potential may effectively lessen the aperture of the contact, thus making the conductance steps sharper and enlarging g [22]. Both mechanisms are consistent with the fact that the negative tails disappear for larger contact length and/or step number, and both processes are likely to occur in different random potential arrangements.

The values of g obtained from the numerical calculations are not quantized, as the expression (32) implies. This is, as stated above, due to the fact that the widths of different quasilocalized states are not exactly the same. Nevertheless, by interpolating this formula to noninteger values of g we achieve a strikingly good description of the numerical results:

$$P_n(g) = \frac{(\kappa L)^{g/\gamma n} \mathrm{e}^{-\kappa L}}{\gamma n \Gamma((g/\gamma n)+1)}. \tag{48}$$

This result can be easily understood, if we take into account that the contribution of each single Q state to the correction to the conductance is small enough (a few per cent of the total effect, see below), so that a comparatively large number of indirect backscattering processes is necessary to obtain the average effect in the QPC. Then the discrete distribution (32) almost coincides with its continuous interpolation (48). This is more true, the longer the contact is. Indeed, the fitting of the two curves is better for the larger values of L (see figure 5).

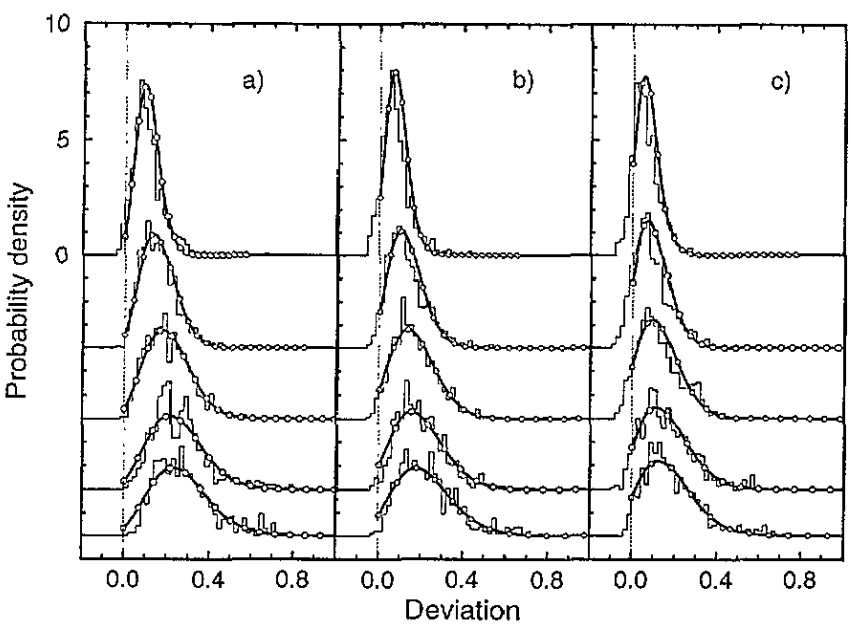

Figure 5. Statistics of conductance fluctuations in QPCs (see text). (a) Contact length 1200 nm, (b) 800 nm, (c) 600 nm.

The solid lines in figure 5 are the least-squares fits of equation (48) to the empirical distribution. The dots on these lines indicate the points where g is an integer multiple of γn (according to (32)). We use the same value of the parameter $\kappa = 1/320\ \mathrm{nm}^{-1} = 0.13/\lambda_F$ for all the curves, while the parameter γ varies (the mean square error of the fitting is in the most cases practically the same as if we varied them both independently). The choice of κ agrees very well with the estimates of section 4 ($\kappa \approx 0.269/\lambda_F \approx 0.006\ \mathrm{nm}^{-1}$), up to a factor of two. This shows that the effective contact length where the scattering occurs is of the order of $L/2$, i.e., coincides with the length of its bottleneck part (see figure 1).

Table 1. Parameter γ as determined by the least-squares fitting of equation (51) to the numerical data for different contact lengths L and step numbers n. Parameter κ is kept equal to 1/320 nm^{-1} for all L, n.

L (nm)	$n=2$	$n=3$	$n=4$	$n=5$	$n=6$	$\bar{\gamma}(L)$
600	0.019	0.018	0.018	0.017	0.016	0.018
800	0.016	0.017	0.017	0.016	0.015	0.016
1200	0.014	0.014	0.014	0.013	0.012	0.014
$\bar{\gamma}(n)$	0.016	0.016	0.016	0.015	0.014	$\langle\gamma\rangle = 0.016$

The values of γ are shown in table 1. They change insignificantly with L and n, and are in a good agreement with the estimates of section 4. The theoretical curves provide a very good description of both the position and magnitude of the distribution peak, as well as of its large deviation tail.

It is noteworthy that the width of the resonant peaks in the $G(V_g)$ curves (figure 3) agrees with our estimates of the resonance width $\Gamma \simeq \gamma n \Delta E_\perp$ ($\Delta E_\perp$ being of the order of the step width).

The knowledge of the distribution function of conductance fluctuations allows us to obtain more accurate criteria of good performance of a QPC, e.g., to predict the probability for a QPC of a given size, realized in the GaAs structure with given properties, to have a certain number of well defined conductance steps.

The analysis of the theory parameters γ and κ shows that for different experimental situations they can be estimated as follows:

$$\gamma \simeq 0.016 \frac{n_{imp}}{n_0} \tag{49}$$

$$\kappa\ (\mathrm{nm}^{-1}) \simeq \frac{1}{320} \exp\left(1 - \frac{n_0}{n_{imp}} \left(\frac{\Delta E_\perp}{\Delta E_{\perp,0}}\right)^2\right). \tag{50}$$

Here n_{imp}, $\Delta E_\perp$ are the actual parameters of the system, and $n_0 = 10^{12}\ \mathrm{cm}^{-2}$, $\Delta E_{\perp,0} = 4.1$ meV [23] are the model parameters in our calculations.

The simplest criterion of the QPC performance is given by the average deviation (see (32))

$$\langle g_n \rangle = \kappa \gamma n L \simeq 5 \times 10^{-5} n L\ (\mathrm{nm}). \tag{51}$$

For the channel length $L = 600$ (800, 1200) nm and for a criterion of total quantization destruction $\langle g \rangle = 0.5$, this gives $n_{max} \approx 17$ (13, 8), respectively. The analysis of conductance curves shows that the quantization is really destroyed at lower values of $\langle g \rangle \simeq 0.2$, i.e. $n_{max} \approx 7$ (5, 3), which is close to what we see in figure 3.

The transport and localization lengths can be estimated from (51) as follows:

$$l_{tr} \approx (\kappa\gamma n)^{-1} \qquad l_{loc} \geqslant l_{tr} n.$$

This leads to the following results: for n open modes $l_{tr} \approx 20\,000/n$ (nm); $l_{loc} \geqslant 20\,000$ (nm). These values are much larger than experimentally reasonable contact lengths; they justify our theoretical approach of section 2.

In the recent experiment [16] quantized conductance was observed in an InAs/AlSb ballistic constriction with channel length 1000 nm. Up to eight conductance steps were detected. Koester *et al* [16] suggest that the much better performance of their device compared to ones utilizing GaAs/$Al_xGa_{1-x}As$ heterostructures is due to a higher ratio of interlevel energy spacing to the amplitude of the impurity potential fluctuations. This is in complete agreement with our theory, since the density of quasilocalized states (and the parameter κ of the theory, see equation (40)) exponentially drops with growing $\Delta E_\perp/\sigma$.

7. Conclusion

In conclusion, we have investigated the effects of electronic scattering by the soft impurity potential in quantum point contacts both with use of an analytical model and by direct numerical calculations.

We have shown that the decisive mechanism of conductance quantization breakdown is due to the indirect backscattering of carriers via quasilocalized states at the Fermi level. For realistic contact lengths they can be described in terms of independent scatterers, though the electron propagation is coherent. This is due to the smoothness of the scattering potentials, leading to very large scattering and localization lengths.

The performance of the quantum contact is shown to be strictly dependent on the ratio of the intermode distance to the amplitude of the random impurity potential (the larger the better).

For the first time we have obtained analytical and empirical formulas both for the conductance deviation due to this process and for the probability distribution of these deviations in an ensemble of contacts with realistic potentials. The latter has proved to be a generalized Poisson distribution.

The parameters of the distribution obtained numerically agree quite well with analytical calculations based on general assumptions, thus confirming their applicability to the case of quantum transport through the QPC in the presence of the random impurity potential.

Acknowledgments

We are grateful to Mats Jonson and Ilya Krive for fruitful discussions. This work was supported by NFR and NUTEK.

References

[1] van Wees B J, van Houten H, Beenakker C W J, Williamson J G, Kouwenhoven L P, van der Marel D and Foxon C T 1988 *Phys. Rev. Lett.* **60** 848
Wharam D A, Pepper M, Ahmed H, Frost J E F, Hasko D G, Peacock D C, Ritchie D A and Jones G A C 1988 *J. Phys. C: Solid State Phys.* **21** L209

[2] Washburn S and Webb R A 1992 *Rep. Prog. Phys.* **55** 1311

[3] Glazman L I, Lesovik G B, Khmel'nitskii D E and Shekhter R I 1988 *Pis'ma Zh. Eksp. Teor. Fiz.* **48** 218 (Engl. Transl. 1991 *JETP Lett.* **48** 238)

[4] Nixon J A and Davies J H 1990 *Phys. Rev.* B **41** 7929
Laughton M J, Barker J R, Nixon J A and Davies J H 1991 *Phys. Rev.* B **44** 1150
Nixon J A, Davies J H and Baranger H U 1991 *Phys. Rev.* B **43** 12638
[5] Büttiker M 1990 *Phys. Rev.* B **41** 7906
[6] Brataas A and Chao K A 1993 *Mod. Phys. Lett.* B **7** 1021
[7] Zagoskin A M and Shekhter R I 1994 *Phys. Rev.* B **50** 4909
[8] Song He and Das Sarma S 1993 *Phys. Rev.* B **48** 4629
[9] Maslov D L, Barnes C and Kirczenow G 1993 *Phys. Rev. Lett.* **70** 1984
[10] Glazman L I and Jonson M 1991 *Phys. Rev.* B **44** 3810
[11] They are only *quasi*localized, since their total energy can be equal to or exceed the energy of propagating states; see below.
[12] Gurvitz S A and Levinson Y B 1993 *Phys. Rev.* B **47** 10578
[13] In the following considerations we neglect the universal conductance fluctuations in the disordered banks of the contact. The reason is that their contribution to the QPC conductance fluctuations is of the order of $(n/N)(2e^2/h) \ll 2e^2/h$ (see [9, 14]), where n is the number of modes in the constriction and N that in the bank. In a typical experimental situation the ratio n/N can be estimated from above by the ratio of the maximum constriction width to the elastic scattering length in the bulk, $d/l_e \leqslant 0.03$ [15]. As we shall see, the above contribution is much less than the characteristic conductance fluctuations due to the mechanisms investigated in our paper.
This is consistent with the experimentally established strong dependence of quality of the conductance quantization on the material, shape, length and intermode spacing in the constriction ([15, 16]), which cannot be due to the *universal* conductance fluctuations in the bulk 2DEG.
[14] Maslov D L, Barnes C and Kirczenov G 1993 *Phys. Rev.* B **48** 2543
[15] Timp G 1991 *Mesoscopic Phenomena in Solids* ed B L Altshuler, P A Lee and R A Webb (Amsterdam: Elsevier) p 273
[16] Koester S J, Bolognesi C R, Hu E L, Kroemer H and Rooks M J 1994 *Phys. Rev.* B **49** 8514
[17] Imry J 1986 *Directions in Condensed Matter Physics* ed G Grinstein and G Mazenko (Singapore: World Scientific) p 101
[18] Wu T-Y and Omura T 1962 *Quantum Theory of Scattering* (Englewood Cliffs, NJ: Prentice-Hall)
[19] Lifshitz I M, Gredeskul S A and Pastur L A 1988 *Introduction in the Theory of Disordered Systems* (New York: Wiley)
[20] Patel N K, Nicholls J T, Martín-Moreno L, Pepper M, Frost J E F, Ritchie D A and Jones G A C 1992 *Phys. Rev.* B **44** 13549
[21] Buckingham M J 1983 *Noise in Electronic Devices and Systems* (New York: Ellis Horwood)
[22] Zagoskin A M and Kulik I O 1990 *Sov. J. Low Temp. Phys.* **16** 533
Bogachek E N, Zagoskin A M and Kulik I O 1990 *Sov. J. Low Temp. Phys.* **16** 796
[23] In fact, the value of $\Delta E_\perp = 4.1$ meV coincides with the distance directly measured in [20] between the first and second transverse modes, which ranged from 4.0 to 4.6 meV for different gate voltages.